Supplementary Material 1 to "A Self-Replicating Radiation-Shield for Human Deep-Space Exploration: Radiotrophic Fungi can Attenuate Ionizing Radiation aboard the International Space Station"

A. Background on *Cladosporium sphaerospermum*

Cladosporium sphaerospermum, a melanized, radiotrophic fungus, characterized chiefly by its ability to utilize ionizing radiation for metabolic functions, was originally discovered in 1886 by Albert Julius Otto Penzig[1]. It is known to be saprotroph, xerotolerant and halotolerant; radiotropism, however, was first discovered following the disaster at the Chernobyl nuclear power-plant, when investigating dematiaceous fungi thriving in the surrounding highly radioactive environment[2]: fungal samples taken from Chernobyl that were exposed to radiation levels approximately 500-times higher than background level, were observed to grow considerably (up to three times) faster than those not exposed to radiation[3]. These organisms continued to grow in the direction of the radiation, another indication for the active pursuit of the radiation as energy-source and thus radiotropism[4]. Radiosynthesis is perceived analogous to photosynthesis, except that where the intricacies of photosynthesis have been extensively studied and are well understood, radiosynthesis remains mostly uncharted territory. While the exact mechanisms of radiotropism remain elusive, it has been found that radiation alters the chemical properties of melanin, which leads to increased rates of electron-transfer, allowing for a net energy-gain[5]. The pigment melanin may thus act in a manner similar to the chlorophyll in photosynthesis, providing energy to be used to reduce carbon. Unlike melanocytes in humans, the melanin is crystallized on the cell-walls of the fungi[6]. This provides protection of the cells from oxidizing agents generated by different forms of ionizing and non-ionizing radiation (ultraviolet light), giving it an evolutionary advantage in extreme natural and non-natural environments on Earth. The expectation is that these properties may also prove advantageous in a Space environment. Therefore, analogous to an existing Earth-based study[4], *C. sphaerospermum* was selected as the subject of an experiment on the International Space Station (ISS).

B. Methodology and Experiment

<u>Absorption Spectrum of Geiger-Counters and Measured Radiation-Levels</u>

Ionizing cosmic radiation, or in other words radiation with enough kinetic or electromagnetic energy to strip electrons from an atom, comes in two forms (excluding photons from the classification): wave radiation (electromagnetic waves) and particle radiation, like alpha- and beta-particles, as well as HZE ions. In the electromagnetic spectrum, ionizing (wave-)radiation is characterized by energies ranging from a few hundred eV to about 1 MeV. The PocketGeiger Type5 measures only wave radiation, specifically of X- and gamma-rays (the X100-7 SMD (First Sensor AG, Berlin, Germany) is sensitive at 23°C for gamma-radiation with energies of 3-20 keV, with highest absorbance between 5.5 keV and 10 keV)[7].

Based on the total cumulative recorded counts over the 30 days of the experiment a recorded dose equivalent around 1 µSv/h (with a correlation between counts and radiation dose for the PocketGeiger Type5 of 4 CPM ≈ 0.075 ± 0.025 µSv/h)[7] was estimated. Given additional shielding due to housing, etc. and considering the narrow absorption spectrum of the Geiger counters, this seems plausible, as it is within one order of magnitude of reported radiation levels on the ISS (≈ 144 µSv/a ≙ 16.44 µSv/h[8], which is to the largest part owed to high-energy nuclei, the most energy-intense fraction of Galactic Cosmic Radiation)[8].

Flight Hardware

The flight-hardware was packaged as a 2U (double standard-size) CubeLab™ (sealed) module (4”×4”×8”), which has a volume of 103.4 in³, is air-tight, and provides up to 20W of power. The assembled unit is shown in figure S1.

Figure S1*:* Fabricated flight hardware unit, packaged in a 2U Space Tango CubeLab™. Media Courtesy: Space Tango, Inc.

The assembled flight-hardware was calibrated and vetted before flight, in particular consistency of the two Geiger counters was confirmed, so that no deviation existed between them. Furthermore, it was ensured that no fungal growth would occur prior to activation (t_0) while enroute to the ISS, by means of cold-stow during transport. On orbit the unit was oriented in a way that the Petri dish faced away from Earth.

C. On-Orbit Growth

Growth of *C. sphaerospermum* was characterized based on the relative brightness of a representative section in photos of the culture in a Petri dish. These sections (on average 350 by 350 pixels of the fungus-side) were cropped from the rest of the photo, and the average color of each crop was determined in hexadecimal values. The values were then converted to decimal values, yielding a relative brightness-level as a numerical measure for the fungal growth in the Petri dish. The values were standardized to $t_0 = 0$, normalized to $t = 48$ h as maximum (cf. supplementary file 2) and plotted over time, yielding a relative growth curve, as shown in figure S2.

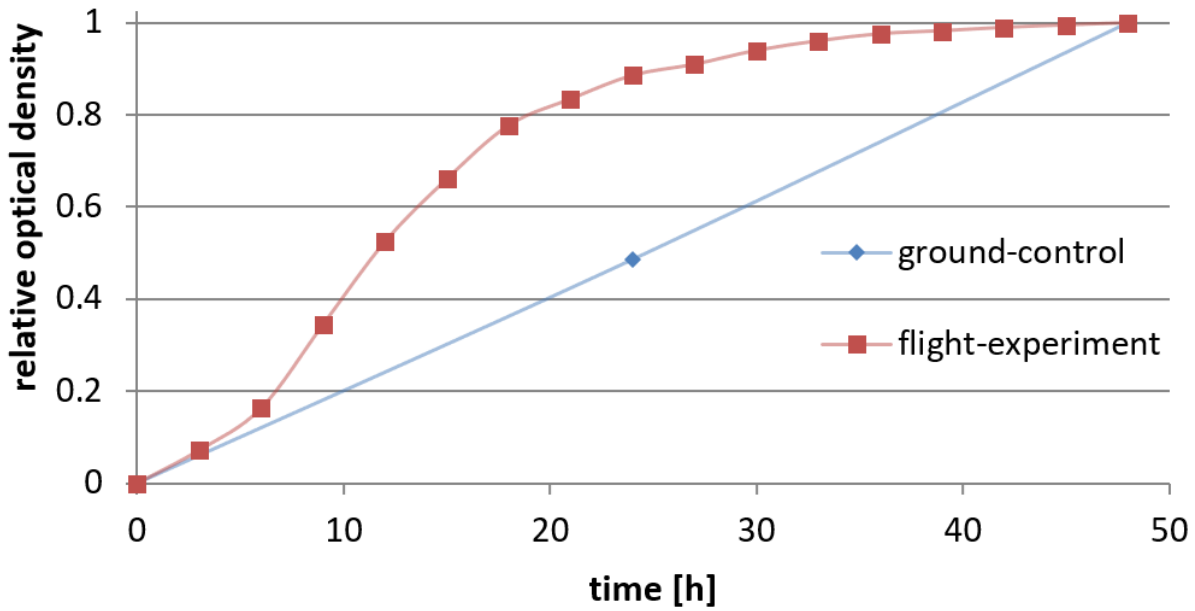

Figure S2: Growth curves for *C. sphaerospermum* on PDA. For the on-orbit experiment (red) the first 48 h are shown in intervals of 3 h, deducted from graphical data (optical density scale normalized to 1 = maximum growth). Due to the few data points for the ground-control (blue), only a qualitative comparison is possible.

While for the on-orbit experiment pictures were taken every 30 min., the ground-control was based on cultures from the cold-stow test with one picture taken each day. Further, the ground-control was grown at an ambient temperature of 26°C, opposed to the on-orbit experiment, which equilibrated at 31.5°C. It has been shown though that up to a relative humidity of 76% there is no significant difference in the growth rate of several fungi, cultivated at 20°C and 30°C[9]. At 98% relative humidity, the rate of growth is roughly[1] 1.2-times (and never more than 1.3-times) as high at 30°C as compared to 20°C. Since in the current experiment the plates were sealed with parafilm, mass transport of damp can be assumed to be limited and therefore the air inside the plate to be saturated. Over 48 hours this could lead to a difference of 8 hours, which is, however, insignificant in the magnitude of discernible difference between growth times for the ground-control and the flight-experiment as in figure S2. Further, *C. sphaerospermum* has a reported optimum temperature of 25°C, with an upper limit of 35°C[10]. Thus, it becomes more likely that at 31.5°C no growth advantage exists over 26°C.

D. Linear Attenuation Coefficients

Background and Definition

A linear attenuation coefficient (LAC, symbol "μ") is a constant, given in per unit thickness of a material and describes the fraction of attenuated incident photons in a monoenergetic beam[11]. Therefore, it can be used to determine the probability that ionizing electromagnetic radiation will be scattered by a material, scaled on a linear attenuation index. An LAC is a material-intrinsic property and describes the ability of a material to shield against radiation, measured in change in energy levels per density multiplied by width. It takes into account initial and final radiation levels, as well as the thickness of the material and its density, to determine the probability that individual atoms within the material will scatter energy waves.

[1] average for the five fungi (*A. candidatus*: ~ 1.05×, *A. flavus*: ~ 1.15×, *A. fumigatus*: ~ 1.24×, *P. fellutanum*: ~ 1.13×, *P. islandicum*: ~ 1.3×), as derived from figure 1 of the respective study[9].

Calculations based on LACs were used to interpret the results gathered in the experiment and put them into perspective.

Equations for LAC Calculations

Eq. 1 $I = I_0 e^{-(\mu/\rho)x}$

Eq. 2 $\mu_m = \sum w_i \left(\frac{\mu}{\rho}\right)_i$

where:

- I = intensity at a depth of x cm in keV
- I_0 = original intensity in keV
- x = thickness of material
- w_i = weight fraction of the component material i

The estimated dose equivalents based on the counts-per-minute (CPM) averaged over the whole course of the experiment (cf. section B as well as supplementary file 2), were used in the following analysis:

- $I_{Control}$ = 0.916 µSv/h
- I_{Exp} = 0.894 µSv/h

With the thickness of the fungal lawn $x \approx 0.167$ cm, only I_0, the ambient radiation levels, inside the lab, remain unknown, in order to be able to determine μ_m of *C. sphaerospermum* (μ_{Csp}), according to Eq. 1. Since $I_{0\text{-Control}} = I_{0\text{-Fungus}}$, $I_{0\text{-Fungus}}$ can be found by plugging $I_{Control}$, $x_{Control}$, and $\mu_{Control}$ into Eq. 1. The control is constituted of a polystyrene (PS) Petri dish, PDA agar and air, and therefore is composed of three independent linear attenuation coefficients. The linear attenuation coefficient of the air in the Petri dish between the PDA agar and the top lid of the Petri dish is negligible, therefore the working LAC for the Petri dish and PDA as a whole can be calculated as follows.

1. *Step 1 – find $\mu_{Control}$*

With a density of PS of 1.05 g/cm^3 and a 2.2 mm wall strength of the Petri dish, as well as density of the medium of 1.036 g/cm^3 (water + 39 g/L PDA) and 13.33 mm average depth, any given 1 cm^2 cross section of the control dish consists of 2×0.231 g PS (Petri dish lid and base) and 1.378 g PDA agar, resulting in a total mass of 1.84 g of the 1 cm^2 cross section. With linear attenuation coefficients of both PDA and PS retrieved from the NIST-XCOM database[12] (for PDA relative percent masses of water, agar, glucose and starch of 96.235%, 1.448%, 1.931% and 0.386% were used, respectively), the cumulative linear attenuation coefficient of the control can be determined with Eq. 2, where w_i is the weight fraction of the component material i:

$$\mu_{\text{Control}} = \frac{1.378\ g}{1.840\ g}(0.0679\ cm^{-1})_{\text{PDA}} + \frac{0.462\ g}{1.840\ g}(0.0762\ cm^{-1})_{\text{Polystyrene}} = 0.0699\ \text{cm}^{-1}$$

Now knowing the cumulative linear attenuation coefficient for the control, $\mu_{Control}$, it can be plugged into Eq. 1 along with $I_{xControl}$ = 0.916 μSv/h, and the total thickness of the Petri dish, to determine the initial radiation levels inside the lab, I_0.

2. *Step 2 – find I_0*

$$0.916\ \mu Sv/h = I_0\, e^{-0.0699\times 1.773} \Leftrightarrow I_0 = 1.034\ \mu Sv/h$$

With I_0, the LAC for the experimental side can be determined. I_{xExp} = 0.894 µSv/h, represents the (attenuated) radiation passing through the fungus, the Petri dish, and the agar. However, the working I_x value solely for *C. sphaerospermum* ($I_{xFungus}$) must be isolated to remove the influence caused by the Petri dish and the PDA agar. This can be done by subtracting the ΔµSv/h of the control side from the ΔµSv/h of the fungus side to find the change in radiation solely caused by the fungus ($_{\Delta}I_{Fungus}$), which can then be subtracted from I_0 to find $I_{xFungus}$.

3. *Step 3 – derive $I_{xFungus}$*

$$(I_0 - I_{xExp}) - (I_0 - I_{xControl}) = {}_{\Delta}I_{Fungus}$$
$$\Leftrightarrow I_0 - {}_{\Delta}I_{Fungus} = I_{xFungus}$$

With integers ⇒ (1.034 µSv/h – 0.894 µSv/h) – (1.034 µSv/h – 0.916 µSv/h) = 0.022 µSv/h
$$\Leftrightarrow 1.034\ \mu Sv/h - 0.022\ \mu Sv/h = 1.012\ \mu Sv/h$$
$$\Leftrightarrow I_{xFungus} = 1.012\ \mu Sv/h$$

Therefore, the final level of radiation attenuated solely by *C. sphaerospermum* lead to a decrease in dose equivalent from 1.034 µSv/h to 1.012 µSv/h.

4. *Step 4 – determine μ_{Fungus}*

By finding an approximated value for I_x, valid for the fully matured fungus, the LAC of *C. sphaerospermum* "μ_{Fungus}" can be derived according to Eq. 1 with I_0, as calculated for the control, and a maximum thickness x of the fungal lawn:

- I_0 = 1.034 µSv/h
- $I_{xFungus}$ = 1.012 µSv/h
- x = 0.167 cm

$$1.012\ \mu Sv/h = 1.034\ \mu Sv/h \times e^{-\mu\times 0.167}$$
$$\Rightarrow \mu_{Fungus} = 0.129\ cm^{-1}$$

Since the fungal lawn shields only one side of the Geiger counter from radiation, the LAC of the fungus can be doubled, giving $\mu_{Fungus}\times 2 = 0.258\ cm^{-1}$ as the effective attenuation capacity.

5. *Step 5 – estimate melanin content of the biomass*

Beyond being a measure of this fungus' ability to shield against ionizing radiation, the LAC of *C. sphaerospermum* can be used to estimate its melanin content, using Eq. 2 and an assumption for the molecular composition of the biomass without melanin:

$$\mu_m = \frac{m}{1\ g}\left(\frac{\mu}{\rho}\right)_{Melanin} + \frac{1-m}{1\ g}\left(\frac{\mu}{\rho}\right)_{Biomass}$$

with:

- m = mass of melanin in a 1 g fungal sample
- $\left(\frac{\mu}{\rho}\right)$= MACs for melanin and fungal biomass, retrieved from NIST-XCOM. The composition of biomass without melanin was the empirical formula of a non-melanized fungus[13].

Evaluated with MACs at 5.5 keV and 10 keV, the boundary energies of the optimal absorption range of the Geiger counter (cf. section B), a range of the melanin content can be determined:

5.5 keV $0.258\ \text{cm}^{-1} = \frac{m}{1\ g}(0.4044\ \text{cm}^2\text{g}^{-1}) + \frac{1-m}{1\ g}(0.1644\ \text{cm}^2\text{g}^{-1}) \Leftrightarrow m = 0.39\ \text{g}$

10 keV $0.258\ \text{cm}^{-1} = \frac{m}{1\ g}(0.3392\ \text{cm}^2\text{g}^{-1}) + \frac{1-m}{1\ g}(0.1926\ \text{cm}^2\text{g}^{-1}) \Leftrightarrow m = 0.44\ \text{g}$

The melanin content of *C. sphaerospermum*, under the given cultivation conditions aboard the ISS can therefore be reported to be within a range of approximately 39% to 44% [w/w].

E. Linear Attenuation - Case Study

The integration of microbial melanin with compounds through chelating of certain metals can effectively increase the overall attenuation capability of the composite material in high-stress gamma-ray environments[14]. However, in an ISRU scenario, the attenuation capability of a melanin composite is most effectively analyzed when combined with regolith. Let material X represent an equimolar mixture of melanin and Martian regolith, such that its linear attenuation coefficient at 100 MeV, μ_X, would be 0.3965 cm^{-1}, according to the NIST-XCOM database[12]. Therefore, Eq. 1 can be written in a way that it expresses the ability of material X to lower the dose equivalent of Martian radiation levels to those on Earth (230 mSv/a → 6.2 mSv/a)[15,16] as follows, where x represents material thickness:

$$0.62/8 = e^{-0.3965 \times x}$$

In this scenario, the required thickness of material X is 9.11 cm. Were regolith replaced with Stainless Steel 301 (LAC @ 10MeV: 1.1954), this would lower to 1.45 cm, whereas the required thickness of melanized fungal biomass (40% melanin [w/w], LAC: 0.1736 cm^{-1}) would be 20.82 cm.

While these calculations based on linear attenuation allow an initial appraisal of the shielding capacity under the given circumstance and subject to the described parameters, they do not holistically describe the real (off-)world radiation environment, due to the complex nature of GCR and vicissitude of space weather. To precisely study the shielding properties of melanin containing materials, tools like OLTARIS[17] and SPENVIS[18] and/or Monte Carlo simulations[19,20] (using a platform like e.g. GEANT4 and CREME96)[21] could model and further validate findings, however, this is out of the scope of this study. This needs to go hand-in-hand with experimental studies and a deeper understanding of the health risk that space radiation poses for human crews[22,23].

F. Data Confidence

For Geiger counters and dosimeters alike, the percent error of the measurements can change when the radiation levels change, as can be seen by reference to the radiation count vs. noise signal plot (supplementary file 2). Because of indeterminable error, an average percent error is assigned to instruments like the sensor used in this experiment. However, since the consistency of the two Geiger counters was confirmed prior to flight, and with ~ 24k data points collected over 720 h of the experiment and a R^2 of the trendlines > 0.99, any relative error can be neglected. Hence, the determined 2.17±0.35% of attenuation is accurate. However, the assumption that radiation intensity on the ISS is not dependent on a vector, may involve an error, as the ISS does not "spin" while orbiting, so that the "bottom" facing Earth may receive a different radiation dose than the "top". Therefore, the true attenuation capacity may be between 1.82% (2.17-0.35%) and 5.04% (4.34+0.7%).

G. Expanded Discussion on ISRU

One possible application of ISRU on Mars is to leverage existing resources in order to increase availability of habitation, in order to significantly reduce the required haul of construction material from Earth as well as to break the supply chain and provide independence as well as redundancy. For this, a multitude of different approaches exists, many of them are still inhibited by the extent of initially required critical infrastructure[24,25]. More recently, autonomous 3D-printing of infrastructure relying on composites with Martian regolith has been proposed[26], but this still requires significant up-mass to strip and process Martian topsoil, as well as the raw material for the binding resin. However, if the binding material could also be derived on-site, an additive manufacturing method may become immediately more feasible.

A passive shield that is both lightweight and an effective attenuator for GCR would significantly contribute to a solution for radiation shielding on Mars, allowing for large yet open Martian habitats to be developed, when looking to establish a permanent foothold on the fourth rock from the sun. While bio-based methods are still in early stages of development, fungal structures have already been targeted by NASA through investigation of mycotecture as a potential technology for production of structural components[27]. Further expanding the range of fungi being tested for growth on regolith simulants would yield information on the feasibility of *C. sphaerospermum* composites based on ISRU to bolster radiation shielding capacity of bio-based habitation. Ultimately "Engineered Living Materials" (ELMs)[28] may provide the game-changing solution for the most pressing issues of deep-space exploration (up-mass and radiation), allowing the tailored construction of structural and supporting components, possibly in combination with 3D bioprinting, which has been shown to be feasible also with fungal mycelium[29].

In future, manufacturing of "melanin-infused" ceramics and alloys, into spacecraft, may increase attenuation capability while keeping the thickness and weight of a material relatively constant. In place of increasing thicknesses of materials such as steel or aluminum, which would result in substantial increase of mass (~ 7 g/cm^3 for standard steel at Earth gravity), the same thicknesses of materials could be "reinforced" with melanin, woven in with melanin as with fabrics. The possibility to polymerize melanin itself[30] may even allow the development of advanced high-performance (plastic) materials.

H. References

1. Bensch, K., Braun, U., Groenewald, J. Z. & Crous, P. W. The genus *Cladosporium*. *Stud. Mycol.* **72**, 1–401 (2012).
2. Karpenko, Y. V., Redchitz, T. I., Zheltonozhsky, V. A., Dighton, J. & Zhdanova, N. N. Comparative responses of microscopic fungi to ionizing radiation and light. *Folia Microbiol. (Praha)* **51**, 45 (2006).
3. Dadachova, E. & Casadevall, A. Ionizing Radiation: how fungi cope, adapt, and exploit with the help of melanin. *Curr. Opin. Microbiol.* **11**, 525–531 (2008).
4. Zhdanova, N. N., Tugay, T., Dighton, J., Zheltonozhsky, V. & Mcdermott, P. Ionizing radiation attracts soil fungi. *Mycol. Res.* **108**, 1089–1096 (2004).
5. Dadachova, E. *et al.* Ionizing Radiation Changes the Electronic Properties of Melanin and Enhances the Growth of Melanized Fungi. *PLOS ONE* **2**, e457 (2007).
6. Eisenman, H. C. & Casadevall, A. Synthesis and assembly of fungal melanin. *Appl. Microbiol. Biotechnol.* **93**, 931–940 (2012).
7. Pocket Geiger Radiation Sensor - Type 5 - SEN-14209 - SparkFun Electronics. https://www.sparkfun.com/products/14209. Web 01 Jul. 2020
8. Cucinotta, F. A., Kim, M.-H. Y., Willingham, V. & George, K. A. Physical and Biological Organ Dosimetry Analysis for International Space Station Astronauts. *Radiat. Res.* **170**, 127–138 (2008).
9. Mannaa, M. & Kim, K. D. Effect of

Temperature and Relative Humidity on Growth of *Aspergillus* and *Penicillium* spp. and Biocontrol Activity of *Pseudomonas protegens* AS15 against Aflatoxigenic *Aspergillus flavus* in Stored Rice Grains. *Mycobiology* **46**, 287–295 (2018).
10. Zalar, P. *et al.* Phylogeny and ecology of the ubiquitous saprobe *Cladosporium sphaerospermum*, with descriptions of seven new species from hypersaline environments. *Stud. Mycol.* **58**, 157–183 (2007).
11. Linear attenuation coefficient | Radiology Reference Article | Radiopaedia.org. https://radiopaedia.org/articles/linear-attenuation-coefficient. Web 01 Jul. 2020
12. curtis.suplee@nist.gov. XCOM: Photon Cross Sections Database. *NIST* https://www.nist.gov/pml/xcom-photon-cross-sections-database (2009). Web 01 Jul. 2020
13. Battley, E. H. An empirical method for estimating the entropy of formation and the absolute entropy of dried microbial biomass for use in studies on the thermodynamics of microbial growth. *Thermochim. Acta* **326**, 7–15 (1999).
14. El-Bialy, H. A., El-Gamal, M. S., Elsayed, M. A., Saudi, H. A. & Khalifa, M. A. Microbial melanin physiology under stress conditions and gamma radiation protection studies. *Radiat. Phys. Chem.* **162**, 178–186 (2019).
15. Mars' Surface Radiation Environment Measured with the Mars Science Laboratory's Curiosity Rover | Science. https://science.sciencemag.org/content/343/6169/1244797. Web 01 Jul. 2020
16. ANS / Public Information / Resources / Radiation Dose Calculator. https://ans.org/pi/resources/dosechart/msv.php. Web 01 Jul. 2020
17. OLTARIS Home Page. https://oltaris.nasa.gov/. Web 01 Jul. 2020
18. SPENVIS - Space Environment, Effects, and Education System. https://www.spenvis.oma.be/. Web 01 Jul. 2020
19. Vuolo, M. *et al.* Monte Carlo simulations for the space radiation superconducting shield project (SR2S). *Life Sci. Space Res.* **8**, 22–29 (2016).
20. Lund, M. & Jevremovic, T. Enhanced GEANT4 Monte Carlo simulations of the space radiation effects on the International Space Station and Apollo missions using high-performance computing environment. *Acta Astronaut.* **165**, 219–228 (2019).
21. Falzetta, G., Longo, F. & Zanini, A. GEANT4 and CREME96 comparison using only proton fluxes. *ArXiv07122149 Phys.* (2008).
22. Chancellor, J. C. *et al.* Limitations in predicting the space radiation health risk for exploration astronauts. *Npj Microgravity* **4**, 1–11 (2018).
23. Life | Free Full-Text | Space Radiation: The Number One Risk to Astronaut Health beyond Low Earth Orbit | HTML. https://www.mdpi.com/2075-1729/4/3/491/htm. Web 01 Jul. 2020
24. Cichan, T. *et al.* Mars Base Camp: An Architecture for Sending Humans to Mars. *New Space* **5**, 203–218 (2017).
25. Gruenwald, J. Human outposts on Mars: engineering and scientific lessons learned from history. *CEAS Space J.* **6**, 73–77 (2014).
26. Made In Space | Build Above | Build Above. https://madeinspace.us/. Web 01 Jul. 2020
27. Hall, L. Myco-architecture off planet: growing surface structures. *NASA* http://www.nasa.gov/directorates/spacetech/niac/2018_Phase_I_Phase_II/Myco-architecture_off_planet (2018). Web 01 Jul. 2020
28. Nguyen, P. Q., Courchesne, N.-M. D., Duraj-Thatte, A., Praveschotinunt, P. & Joshi, N. S. Engineered Living Materials: Prospects and Challenges for Using Biological Systems to Direct the Assembly of Smart Materials. *Adv. Mater. Deerfield Beach Fla* **30**, e1704847 (2018).
29. 3D Printing With Fungus - Artist Creates Chairs and Other Objects Out of Mushrooms - 3DPrint.com | The Voice of 3D Printing / Additive Manufacturing. https://3dprint.com/7279/3d-print-fungus-mycelium/. Web 01 Jul. 2020
30. Solano, F. Melanin and Melanin-Related Polymers as Materials with Biomedical and Biotechnological Applications-Cuttlefish Ink and Mussel Foot Proteins as Inspired Biomolecules. *Int. J. Mol. Sci.* **18**, (2017).